Liquid Crystals
Publication details, including instructions for authors and subscription information:
http://www.informaworld.com/smpp/title~content=t713926090

Quantitative analysis of the packing of alkyl glycosides: a comparison of linear and branched alkyl chains

H. S. Nguan[a]; T. Heidelberg[a]; R. Hashim[a]; G. J. T. Tiddy[b]
[a] Department of Chemistry, Faculty of Science, University of Malaya, Kuala Lumpur, Malaya [b] School of Chemical Engineering & Analytical Science, University of Manchester, Manchester, UK

Online publication date: 09 September 2010

To cite this Article Nguan, H. S. , Heidelberg, T. , Hashim, R. and Tiddy, G. J. T.(2010) 'Quantitative analysis of the packing of alkyl glycosides: a comparison of linear and branched alkyl chains', Liquid Crystals, 37: 9, 1205 — 1213
To link to this Article: DOI: 10.1080/02678292.2010.492245
URL: http://dx.doi.org/10.1080/02678292.2010.492245

Liquid Crystals,
Vol. 37, No. 9, September 2010, 1205–1213

Taylor & Francis
Taylor & Francis Group

Quantitative analysis of the packing of alkyl glycosides: a comparison of linear and branched alkyl chains

H.S. Nguan[a], T. Heidelberg[a]*, R. Hashim[a] and G.J.T. Tiddy[b]

[a]*Department of Chemistry, Faculty of Science, University of Malaya, Kuala Lumpur, Malaya;* [b]*School of Chemical Engineering & Analytical Science, University of Manchester, Manchester, UK*

(*Received 2 November 2009; final version received 6 May 2010*)

In an attempt to relate the geometry of glycolipid assemblies with molecular packing constraints, the surface areas per molecule for straight and branched-chain alkyl glycosides with varying chain length are calculated. Effects of temperature, water content, sugar size and paraffin chain length are analysed based on closest packing assumption. The results show a continuous increase of the interface between the hydrophilic and the hydrophobic domain per molecule with growing dominance in bulkiness of either domain, until it reaches a maximum in hexagonal phases. The surface area per molecule, on the other hand, exhibits a sudden jump upon the phase transition from a lamellar to a hexagonal phase, reflecting different values of the packing parameter in both assemblies. This increase is primarily based on the assembly, rather than on molecule-based domain sizes. Therefore, estimations of molecular region sizes can serve only to determine the principal ability of compounds to form certain phases, but not predict the actual phase exhibited under given conditions. Within straight-chain glycosides the surface area per molecule is practically constant, whereas it increases with growing chain length for branched-chain analogues. This can be explained with differences in the volume–length ratio of the hydrocarbon domain.

Keywords: packing; alkyl glycoside; branched chain; geometric analysis; SAXS

1. Introduction

The general structure of alkyl glycosides comprises a hydrophilic sugar head linked to a hydrophobic hydrocarbon chain via a glycosidic bond (Figure 1). Alkyl glycosides are biocompatible surfactants that are readily synthesised from renewable resources, i.e. fatty alcohols and oligosaccharides [1]. They find typical applications as emulsifying agents, especially in cosmetic formulations.

Alkyl glycosides are amphitropic molecules, which means that they can exhibit liquid crystal behaviour both in the absence (thermotropic) and the presence of a solvent (lyotropic), usually water [2]. Several studies on alkyl glycoside mesophases have been published by various authors [3–7]. A range of assembly structures, involving layer (smectic A or lamellar), columnar (usually hexagonal) and cubic phases (bicontinuous and discontinuous) may be obtained. In general, simple glycosides with linear alkyl chains only exhibit the thermotropic smectic A phase [8], while branched chain alkyl glycosides may form a variety of liquid crystal phases such as smectic A, reversed hexagonal and bicontinuous cubic phases, depending on criteria such as the chain length, size of the head group and temperature [6]. Despite various investigations on alkyl glycosides, the packing descriptions of the aggregates from X-ray studies have so far only been rather qualitative. They have not considered the detailed molecular packing to quantify the shape of the glycolipids as reflected in the average head group areas and lengths of the alkyl chains. These parameters have been found to be fundamental in the description of mesophase formation by conventional surfactants [9].

Table 1 illustrates the thermotropic phase behaviour of a range of structurally diverse glycolipids. The data clearly demonstrate the difference between single (straight)-chain glycosides and branched-chain analogues; while the first only form layer-type smectic phases, the latter can exhibit a wider phase diversity that may involve polymorphism, i.e. the formation of various liquid crystalline phases at different temperature ranges. However, a minimum length of the branched chain is required to deviate from the behaviour of straight glycosides. The long branched-chain glycosides exhibit increasing stability for a columnar phase, while shorter analogues only show the lamellar smectic A phase.

These observations suggest that the formation of the smectic A phase is largely stabilised by the extensive attractive interactions within the head group of the glycolipids. Increasing sugar size, i.e. a disaccharide (e.g. maltose) instead of a monosaccharide (e.g. glucose), increases the smectic A stability; hence, all maltosides exhibit a smectic A phase, unlike the corresponding glucosides. The inverse columnar phase, on the other hand, is driven by the branched hydrophobic chain. Conclusively, long branched-chain glucosides only exhibit columnar assemblies. For branched-chain maltosides

*Corresponding author. Email: heidelberg@um.edu.my

ISSN 0267-8292 print/ISSN 1366-5855 online

DOI: 10.1080/02678292.2010.492245
http://www.informaworld.com

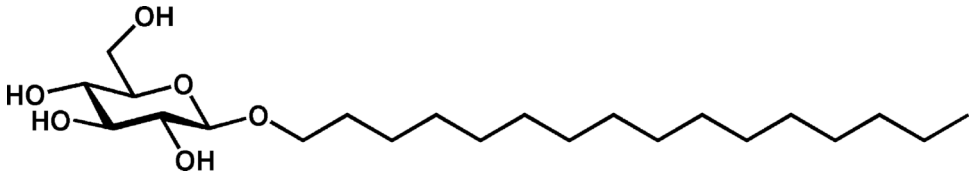

Figure 1. Structural formula of typical alky glycoside (β-cetyl glucoside).

Table 1. Phase behaviour of anhydrous alkyl glycosides; Glc = glucose, Gal = galactose, Man = mannose, Malto = maltose, cello = cellobiose, Cr = crystalline, S_A = smectic A, Cub = bicontinuous cubic, H_{II} = inverse columnar, Iso = isotropic.

Glycolipid	Chain type	Phases	Ref
$\alpha GlcOC_8$	Straight	Cr 69°C S_A 116°C Iso	[3]
$\alpha GlcOC_{18}$	Straight	Cr 98°C S_A 151°C Iso	[4b]
$\beta GlcOC_8$	Straight	Cr 69°C S_A 107°C Iso	[3]
$\beta GlcOC_{12}$	Straight	Cr 80°C S_A 143°C Iso	[4b]
$\beta GlcOC_{18}$	Straight	Cr 93°C S_A 147°C Iso	[4b]
$\beta GlcOC_6 2C_2$	Branched	Cr(?) S_A 55°C Iso	[6a]
$\beta GlcOC_8 2C_4$	Branched	Cr(?) S_A 57°C Iso	[6a]
$\beta GlcOC_{10} 2C_6$	Branched	Cr(?) H_{11} 62°C Iso	[6a]
$\beta GlcOC_{12} 2C_8$	Branched	Cr(?) H_{11} 72°C Iso	[6a]
$\beta GlcOC_{14} 2C_{10}$	Branched	Cr(?) H_{11} 95°C Iso	[6a]
$\alpha GalOC_{18}$	Straight	Cr 89°C S_A 146°C Iso	[4b]
$\beta GalOC_8$	Straight	Cr 96°C S_A 127°C Iso	[3]
$\beta GalOC_{12}$	Straight	Cr 99°C S_A 166°C Iso	[4b]
$\beta GalOC_{18}$	Straight	Cr 106°C S_A 164°C Iso	[4b]
$\beta GalOC_6 2C_2$	Branched	Cr(?) S_A 111°C Iso	[6a]
$\beta GalOC_{12} 2C_8$	Branched	Cr(?) H_{11} 116°C Iso	[6a]
$\beta GalOC_{14} 2C_{10}$	Branched	Cr(?) H_{11} 133°C Iso	[6a]
$\alpha ManOC_8$	Straight	Cr 58°C S_A 132°C Iso	[3]
$\alpha ManOC_{10}$	Straight	Cr 62°C S_A 149°C Iso	[3]
$\alpha ManOC_{12}$	Straight	Cr 67°C S_A 157°C Iso	[3]
$\alpha MaltoOC_{12}$	Straight	Cr 80°C 244 S_A	[4a]
$\beta MaltoOC_{12}$	Straight	Cr 80°C S_A 244°C Iso	[4c]
$\beta MaltoOC_{18}$	Straight	Cr 106°C S_A 274°C Iso	[4c]
$\beta MaltoOC_6 2C_2$	Branched	Cr(?) S_A 137°C Iso	[6a]
$\beta MaltoOC_8 2C_4$	Branched	Cr(?) S_A 188°C Iso	[6a]
$\beta MaltoOC_{10} 2C_6$	Branched	Cr(?) S_A 189°C Iso	[6a]
$\beta MaltoOC_{12} 2C_8$	Branched	Cr(?) S_A 115°C Cub 192°C H_{11} 210°C Iso	[6a]
$\beta MaltoOC_{14} 2C_{10}$	Branched	Cr(?) S_A 73°C Cub 131°C H_{11} 225°C Iso	[6a]
$\beta CelloOC_{18}$	Straight	Cr 152°C S_A 284°C Iso	[4c]
$\beta CelloOC_8 2C_4$	Branched	Cr(?) S_A 170°C Cub 176°C Iso	[6a]
$\beta CelloOC_{12} 2C_8$	Branched	Cr(?) S_A 139°C H_{11} 196°C Iso	[6a]
$\beta CelloOC_{14} 2C_{10}$	Branched	Cr(?) H_{11} 235°C Iso	[6a]

with long alkyl chains (12/10 and 14/12) a compromise is observed, leading to mesophase polymorphism. With increasing temperature the structure changes from smectic A to columnar, passing through one or more inverse bicontinuous cubic phase(s).

The thickness of the alkyl glycoside bilayer can be measured by small angle X-ray scattering (SAXS). However, SAXS experiments do not directly provide information on the separations of molecules within the layer, which is important for a more detailed description of the packing structure. This prompted us to investigate the variation of the surface area per molecule from available literature data. Here, we would like to present a quantitative analysis based on a microphase separation model with domain densities represented by the sugar and the alkyl chain of the glycolipid. Based on these results, we attempt to explain the observations indicated above.

For lyotropic mesophases, the packing of the assembly is the result of competition between the interfacial curvature and the chain packing constraint [10]. The self-assembled system tends to curve homogeneously, but can be *frustrated* due to a problem of the hydrocarbon chain to fill the three-dimensional Euclidean space [11]. In general, the assembly of amphiphiles depends on the average molecular geometric shape, which is either conical or cylindrical. This shape factor can be described by using the concept of the packing parameter (p) [12] that was originally derived for lyotropic systems [13]. It is the ratio of the molecular volume of the alkyl chain (v) divided by the product of the surface area per molecule (a) and the radius of the aggregate (r_a). The radius of the micelle can not be longer than the longest all-trans hydrocarbon chain length. As entropy favours the formation of the smallest possible aggregate, for normal micelles, p takes the values:

$$p \leq \frac{1}{3} \text{ spherical micelle;}$$

$$\frac{1}{3} \leq p \leq \frac{1}{2} \text{ hexagonal (circular-rod) micelle;}$$

$$\frac{1}{2} \leq p \leq 1 \text{ bilayer;}$$

$$p \approx 1 \text{ lamellar; } p > 1 \text{ inverse micelle.}$$

The system above has been developed for surfactants in water, where the molecular surface area is commonly dominated by the hydrophilic domain. In order to apply it for oil-dominated systems, the range for $p > 1$ requires a more detailed analysis. For a water-free system it is easy to show that similar calculations give:

$$p \geq 3 \text{ inverse spherical micelle;}$$

$$3 \geq p \geq 2 \text{ inverse hexagonal micelle;}$$

$$2 \geq p \geq 1 \text{ bilayer.}$$

Here the micelle radius is limited by the extended length of the head group, and the volume is that of the head group. When water is present the treatment is no longer valid as the inverse micelle radius is not limited by the fully extended length, with water filling the additional space. Thus the p value does not provide a guide to micelle structure.

2. Methodology

Due to the micro-phase separation in amphiphilic systems, the two different molecular regions are separated from each other. The density of a closest-packed structure without constraints can be estimated based on reference densities of model compounds for each of the domains. For glycolipids these refer to the sugar and the lipid chain. The density of a glycolipid aggregate, ρ_L, can be calculated according to:

$$\rho_L = \frac{M_L}{V_L} = \frac{M_L}{V_C + V_S} = \frac{M_L}{\frac{M_C}{\rho_C} + \frac{M_S}{\rho_S}}, \quad (1)$$

where ρ = density, M = molecular mass and V = volume; the indices L, S and C, refer to glycolipid, sugar head and paraffin chain, respectively.
Therefore:

$$\rho_L = \frac{\rho_S \rho_C M_L}{\rho_S M_C + \rho_C M_S}. \quad (2)$$

Our calculations are based on densities for the sugar head and the paraffin chain as 1.5 g cm^{-3} and 0.8 g cm^{-3}, respectively, at room temperature, referring to experimental data for paraffins [14] and various sugars, like glucose and sucrose [15], which match our experimental value for amorphous maltose. For higher temperatures, thermal expansion will lead to a reduction of the density; the thermal coefficients are $\Delta\rho(T) = -0.06$ g m^{-1} K^{-1} for the sugar [16] and –0.1 g m^{-1} K^{-1} for the paraffin [17]. Applying Equation (1) by replacing the molecular volume by a term based on the layer spacing, d_0, from SAXS measurements, the surface area per molecule for a lamellar system, A_{lam}, can be calculated according to the following equation [18]:

$$A_{lam} = \frac{2M_L}{\rho_L d_0 N_A}. \quad (3)$$

Unlike the case of lamellar cases, where one surface area per molecule is sufficient to describe both molecular surface as well as the interface between molecular domains, two different data apply for columnar assemblies. These are illustrated in Figure 2. The molecular surface area, A_{hex}, takes the shape of a hexagonal cylinder, whereas as the domain interface area, A_{IF}, forms a circular cylinder. The latter requires the consideration of the volume fraction of the non-continuous phase. The two surface areas can be calculated according to:

$$A_{hex} = 2\sqrt{3}\frac{M_L}{\rho N_A d_0}, \quad (4)$$

and

$$A_{IF} = \sqrt{2\pi\sqrt{3}}\sqrt{\varphi}\frac{M_L}{d_0 \rho_L N_A}, \quad (5)$$

with φ = volume fraction of the discontinuous phase, defined by:

$$\varphi = \frac{V_{\text{inner cir.Cyl.}}}{V_{\text{hex.Cyl.}}} = \frac{V_{\text{discont.phase}}}{V_{\text{discont.phase}} + V_{\text{cont.phase}}}. \quad (6)$$

(For derivation of Equations (4) and (5) see supplementary information #1, available via the multimedia link on the online article webpage.) The volumes of the different regions are determined based on the respective molecular domain mass as indicated earlier:

$$V = \frac{M}{\rho}. \quad (7)$$

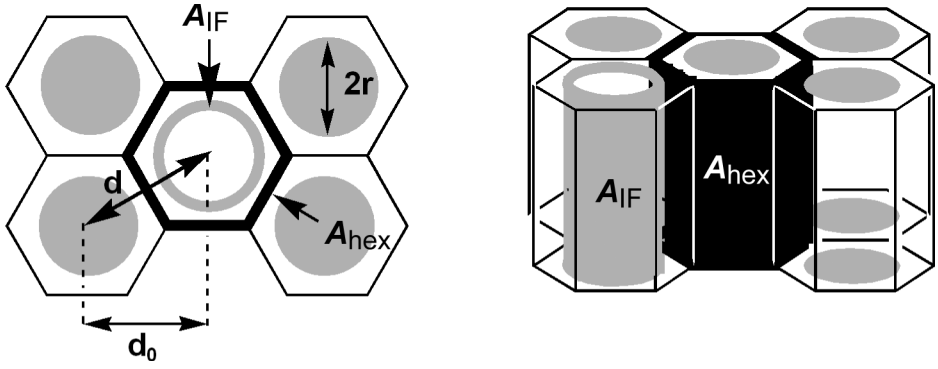

Figure 2. Surface area A_{hex} vs. domain interface area A_{IF} for hexagonal assemblies.

Unlike the molecular domain interface, the surface area per molecule is independent of the relative domain sizes (see Figure 2). It is an important property, since it resembles the surface area of the dominating molecular domain and, therefore, can be used for the calculation of the packing parameter according to:

$$p = \frac{A_{\text{hydrophobic domain}}}{A_{\text{hydrophilic domain}}}. \tag{8}$$

SAXS measurements only provide access to the molecular surface area but not to the surface area of a particular molecular domain. However, the molecular surface area is determined by the dominating molecular domain, thus A can be used to quantify the dominating region. For straight-chain glycosides this is the sugar head. The minimum surface area of a linear paraffin, on the other hand, can be estimated based on an all-trans-oid conformation of the carbon chain. Assuming an average bond length of $d_{C-C} = 1.54$ Å for a carbon–carbon bond, the maximum length of an alkyl chain can be calculated according to:

$$x_{\max}(C_n) = n\ d_{C-C} \sin\left(\frac{109.5^\circ}{2}\right). \tag{9}$$

Since the molecular volume of the model hydrocarbon chain is resembled by the product $x_{\max}$ and the surface area, $A_{\min}$ is accessible from the density of hydrocarbons. Based on an average density of 0.8 g cm^{-1} for a hydrocarbon, the surface area of a straight alkyl chain is estimated as $A_{\text{straight alkyl}} = 23$ Å^2. Due to non-perfect packing in liquid crystal phases the actual value is expected to be slightly higher. However, the calculated value constitutes a reasonable estimation.

While the surface area for a hydrocarbon chain can be estimated relatively simply, based on a geometrical model, a corresponding approach for a sugar head-group in a surfactant is difficult, particularly with respect to configurational effects of the glycosidic bond, which give rise to significantly different sizes of α- and β-glycosides. In order to avoid these complications, a different approach for the determination of packing parameters for branched-chain glycosides is applied. Instead of theory-based data, the SAXS-determined surface area of a straight alkyl chain glycoside, A_0, is used as reference for the surface area of the sugar head-group. This approach is justified, since the sugar domain determines the surface area per molecule for straight-chain glycosides, as indicated above.

In order to rationalise the effect of alkyl branching on the molecular surface area, we compare it with the swelling of glycoside surfactants upon water addition. Increasing surface area for the latter is due to the hydration of the sugar (for illustration, see supplementary information #2, available via the multimedia link on the online article webpage). Unlike previous investigations [18], our calculations of lyotropic systems consider the solvent as an integral part of the polar domain. Therefore, water contributes to the volume and mass of the polar domain. Instead of the sugar density, ρ_S, the density of a sugar-water mixture, ρ_{SW}, is used. Within the concentration range of available SAXS data, we assume a linear relationship between density and concentration, Equation (10), which is supported by experimental results [16]:

$$\rho_{SW} = \rho_S - x_{aq}\left(\rho_S - \rho_{aq}\right), \tag{10}$$

with ρ = density, x = concentration in sugar phase (wt%), aq = water.

The presence of water influences the calculation of the density of the lyotropic system, ρ_{lyo}, which is required instead of ρ_L in Equations (3)–(5). It can be calculated according to Equation (11):

$$\rho_{lyo} = \frac{M_L + m_{aq}}{V_C + V_{SW}}, \tag{11}$$

with $m_{aq} = \frac{c_{aq} M_L}{1 - c_{aq}}$, $V_C = \frac{M_C}{\rho_C}$ and $V_{SW} = \frac{M_S + m_{aq}}{\rho_{SW}}$.
The remaining variable x_{aq}, see Equation (10), can be determined from c_{aq} according to:

$$x_{aq} = \frac{m_{aq}}{M_S + m_{aq}} = \frac{c_{aq} M_L}{M_S(1 - c_{aq}) + c_{aq} M_L}. \tag{12}$$

Besides the molecular surface area, packing parameter and domain interface area per molecule, we determined the thickness of domains for lamellar systems and the diameter of the non-continuous phase cylinders for hexagonal assemblies, respectively. These data are most effective for demonstrating the effects of temperature, chain length and water content on the assembly dimensions. The calculation of all these data requires the volume fraction for either domain. The value for the hydrophobic domain can be obtained by Equation (13):

$$\varphi_C = \frac{V_C}{V_C + V_{SW}} = \frac{\rho_{SW} M_C}{\rho_{SW} M_C + \rho_C\left(M_S + x_{aq} M_L\right)}, \tag{13}$$

whereas the thickness of the hydrophobic domain, d_C, only requires multiplication of the volume fraction with the layer spacing, according to:

$$d_C = \varphi_C \times d_0, \tag{14}$$

the diameter of the core domain of columnar assemblies, $2r$, can be calculated by:

$$2r = \sqrt{\varphi_{\text{discont. phase}}}\, d_0 \sqrt{\frac{8}{\sqrt{3}\pi}}. \qquad (15)$$

3. Results and discussion

Table 1 demonstrates the exclusive formation of a smectic liquid crystalline phase for straight-chain alkyl glycosides, whereas for branched-chain analogues a columnar phase is stabilised with increasing chain length and temperature. The corresponding molecular surface areas are displayed in Tables 2-4. The surface area per molecule for straight chain glycosides (Table 2) appears to be only moderately affected by both temperature (βGlcOC$_8$) and size of the hydrophobic domain (αMan-series), while branched-chain glycolipids show a continuous rise of the surface area per molecule with increasing hydrophobic domain (Tables 3 and 4). Table 4 also indicates an increase of the molecular surface area upon heating of a branched-chain surfactant. Correspondingly, the thickness of the sugar domain, d_s, remains practically constant for straight-chain glycosides, whereas it decreases with increasing hydrophobic domain and temperature for the branched analogues. This demonstrates a significant difference between straight and branched-chain glycosides; while the surface area of the hydrophilic domain dominates the first, it is the hydrophobic domain in the latter. The compression of the sugar region can be explained with a closer packing perpendicular to the layer normal, which is induced by the surface area of the hydrophobic domain. Unlike for the hydrophobic domain, this compression cannot be achieved by conformational changes, because of limited conformational freedom of the sugar based on the cyclic structure. Therefore, either interdigitation of sugar units or a change of the tilt angle of the sugar and layer normal remain the only possibilities. The latter is more likely, since it can accommodate a gradual change of the surface area based on continuous variation of the tilt angle (see supplementary information #3, available via the multimedia link on the online article webpage).

The diameter of the sugar domain in the inverse hexagonal assembly, represented by $2r_S$ in Tables 3 and 4, remains practically constant for compounds comprising the same sugar. This reflects a constant volume requirement of the sugar domain and indicates that the increasing volume demand for the hydrophobic domain can be achieved by simply enlarging the distance between the columns.

The different behaviour of the surface area per molecule for straight and branched-chain glycosides can be explained based on the ratio of the volume and the maximal length of the hydrophobic domain (V_C/x_{max}). Since the volume correlates with the domain's mass, V_c/x_{max} may be replaced by M_C/x_{max} as displayed

Table 2. Surface area per molecule, A, and packing parameter for straight glycolipids. d_0 = repeating distance from SAXS measurements, φ_c = volume fraction of hydrocarbon chain, d_C / d_S = thickness of the hydrophobic / hydrophilic domain.

Glycolipid	T [°C]	d_0 [Å]	Ref	Phase	φ_c	d_c [Å]	d_S [Å]	ρ_1 [g/cm^2]	A [Å^2]	A/A_0
-CH_2-CH_2-			all-transoid; $d_{c\text{-}c}$=1.54Å; ϕ_{ccc}=109.5°					0.8	23	ref.
βGlcOC$_8$	70	25.6	[3]	S_A	55%	14.1	11.5	1.08	35	1.5
	105	25.3	[3]	S_A	56%	14.2	11.1	1.05	37	1.6
βGalOC$_8$	90	25.8	[3]	S_A	56%	14.4	11.4	1.06	36	1.5
αManOC$_8$	90	23.1	[3]	S_A	56%	12.9	10.2	1.06	40	1.7
αManOC$_{10}$	90	26.4	[3]	S_A	61%	16.1	10.3	1.02	40	1.7
αManOC$_{12}$	90	28.9	[3]	S_A	65%	18.9	10.0	0.99	41	1.8
αManOC$_{12}$	50	32.5	[5]	S_A	49%	15.8	16.7	1.14	46	2.0
βManOC$_{12}$	80	41.5	[5]	S_A	49%	20.5	21.2	1.11	37	1.6

Table 3. Surface area per molecule, A, and packing parameter for branched glucosides. d_0 = repeating distance from SAXS measurements, φ_c = volume fraction of hydrocarbon chain, d_C / d_S = thickness of the hydrophobic / hydrophilic domain, $2r_S$ = diameter of sugar cylinder, d = cylinder distance, ρ_1 = density of glycolipid, A_{IF} = interfacial surface area of domains.

Glycolipid	d_0 [Å]	Phase	φ_c	d_c [Å]	d_S [Å]	$2r_s$ [Å]	d [Å]	ρ_1 [g/cm^2]	A_{IF} [Å^2]	A [Å^2]	A/A_0
βGlcOC$_8$	25.6$^{70°c}$	S_A	55%	14.1	11.5	-	-	1.08		35	ref.
βGlcOC$_6$2C$_2$	21.85	S_A	54%	11.8	10.0	-	-	1.12		39	1.1
βGlcOC$_8$2C$_4$	23.29	S_A	64%	14.9	8.4	-	-	1.05		47	1.3
βGlcOC$_{10}$2C$_6$	24.87	H_{11}	70%	-	-	16.5	28.7	1.01	48	92	2.6
βGlcOC$_{12}$2C$_8$	26.83	H_{11}	75%	-	-	16.4	31.0	0.98	48	101	2.9
βGlcOC$_{14}$2C$_{10}$	28.85	H_{11}	78%	-	-	16.4	33.3	0.95	48	108	3.1

Table 4. Surface area per molecule, A, and packing parameter for branched maltosides. d_0 = repeating distance from SAXS measurements, φ_c = volume fraction of hydrocarbon chain, d_C / d_S = thickness of the hydrophobic / hydrophilic domain, $2r_S$ = diameter of sugar cylinder, d = cylinder distance, ρ_1 = density of glycolipid, A_{IF} = interfacial surface area of domains.

Glycolipid	T [°C]	d_0 [Å]	Phase	φ_c	d_c [Å]	d_s [Å]	$2r_s$ [Å]	d [Å]	ρ_1 [g/cm^2]	A_{IF} [Å^2]	A [Å^2]	A/A_0
βMaltoOC$_{12}$	25	33.5	S_A	48%	16.1	17.4	-	-	1.23		43	ref.
βMaltoOC$_6\beta$C$_2$	25	27.59	S_A	38%	10.6	17.0	-	-	1.24		44	1.0
βMaltoOC$_8\beta$C$_4$	25	29.72	S_A	48%	14.3	15.4	-	-	1.16		49	1.1
βMaltoOC$_{10}\beta$C$_6$	25	31.53	S_A	55%	17.4	14.1	-	-	1.11		53	1.2
βMaltoOC$_{12}\beta$C$_8$	25	36.18	S_A	61%	22.0	14.2	-	-	1.07		53	1.2
	100	34.48	S_A	62%	21.5	13.0	-	-	1.00		60	1.4
	100	34.48	S_A	62%	21.5	13.0	-	-	1.00		60	1.4
	200	34.22	H_{11}	65%	-	-	24.6	39.5	0.90	66	116	2.7
βMaltoOC$_{14}\beta$C$_{10}$	25	36.93	S_A	65%	24.0	12.9	-	-	1.05		58	1.3
	100	36.63	S_A	66%	24.4	12.3	-	-	0.97		63	1.5
	160	35.59	H_{11}	68%	-	-	24.5	41.1	0.91	65	121	2.8

Table 5. Volume length ratio for branched and straight alkyl chains, resembled by the ratio of mass and length χ_{max}.

	Straight chain			Branched chain		
Alkyl domain	Code	X_{max} [Å]	M_C/X_{max} [g mol^{-1} Å^{-1}]	Code	X_{max} [Å]	M_C/X_{max} [g mol^{-1} Å^{-1}]
C_8H_{17}	C_8	10.0	11.3	$C_6$2C_2	7.5	15.0
$C_{10}H_{21}$	C_{10}	12.6	11.2	-		
$C_{12}H_{25}$	C_{12}	15.1	11.2	$C_8$2C_4	10.0	16.8
$C_{14}H_{29}$	C_{14}	17.6	11.2	-		
$C_{16}H_{33}$	C_{16}	20.1	11.2	C_{10}2C_6	12.6	17.9
$C_{18}H_{37}$	C_{18}	22.6	11.2	-		
$C_{20}H_{41}$	C_{20}	25.2	11.2	C_{12}2C_8	15.1	18.6
$C_{22}H_{45}$	C_{22}	27.7	11.2	-		
$C_{24}H_{49}$	C_{24}	30.2	11.2	C_{14}2C_{10}	17.6	19.1

in Table 5. While straight chains show a constant ratio M_C/x_{max}, the corresponding data for branched-chain compounds are steadily increasing. The thermal trend may be explained accordingly based on an entropic effect, which leads to increasing deviation from the all-transoid conformation with rising temperature, thus shortening x while M_C remains constant.

The packing parameter (for better readability the reciprocal value $p^{-1}=A/A_0$ *is* displayed in Tables 2-4) for straight-chain glycosides consistently remains below ½ (Table 2), thus confirming a lamellar, or smectic phase. The only exception to this rule is found in αMaltoOC$_{12}$, which exhibits the value resembling the geometric change of the assembly from lamellar to columnar. However, this discrepancy is based on the underestimation of the molecular surface area for the reference A_0 due to the all-transoid conformation assumption. Branched-chain glycolipids, on the other hand, exhibit a packing parameter varying between 1 and $^1/_3$ (Tables 3 and 4), which corresponds to the geometry of the experimentally found phase.

A comparison of Tables 3 and 4 indicates higher affinity of branched-chain maltosides for lamellar assemblies, compared with glucosides. This correlates with a significantly larger domain interface area of the disaccharide head group. The increase in interface area, however, is substantially smaller than the increase in size of the hydrophilic head group. A look into Table 2 reveals significant differences between interface areas of α- and β-glycosides; α-anomers exhibit larger molecular surface areas, e.g. $\sim$ 40 Å^2 for α-mannosides but only $\sim$ 35 Å^2 for β-glucosides and β-galactosides. These results are consistent with simulation studies on lamellar glycolipid assemblies, which also gave larger layer spacings, reflecting smaller interface areas, for β-anomers [19]. This suggests that the anomeric linkage greatly affects the molecular surface area (for more illustration, see supplementary information #4, available via the multimedia link on the online article webpage). In fact, the increase of molecular surface area from glucose to maltose originates to a major content from the α-(1$\rightarrow$4) glycosidic linkage of the two glucose units.

Table 6 displays experimental data and calculated molecular surface areas for lyotropic glycolipid assemblies. The surface area per molecule rises with increasing

Table 6. Surface area per molecule, A, and packing parameter for lyotropic glycolipid formulations; bold values do not match packing theory predictions. d_0 = repeating distance from SAXS measurements, φ_c = volume fraction of hydrocarbon chain, d_C / d_S = thickness of the hydrophobic / hydrophilic domain, $2r_c$ = diameter of sugar cylinder, d = cylinder distance, ρ_l = density of glycolipid, A_{IF} = interfacial surface area of domains.

Glycolipid	c_{aq} [%]	T [°C]	d_0 [Å]	Ref	Phase	φ_c	d_c [Å]	d_s [Å]	$2r_c$ [Å]	d [Å]	ρ_l [g/cm^2]	A_{IF} [Å^2]	A [Å^2]	A/A_0
-CH_2-CH_2-	all-transoid; $d_{c\text{-}c}$ = 1.54Å; ϕ_{ccc} = 109.5°										0.80		23	ref.
βGlcOC$_8$	5	25	26.6	[3]	L_α	52%	13.7	12.9	-	-	1.12		34	1.5
	19	25	29.7	[3]	L_α	45%	13.3	16.4	-	-	1.10		35	1.5
	33	25	33.3 d = 38.6	[3]	H_1	39%	-	-	25.2	38.6	1.06	37	63	2.7
βGalOC$_8$	8	50	26.5	[3]	L_α	51%	13.4	13.1	-	-	1.09		36	1.6
	13	50	28.2	[3]	L_α	48%	13.6	14.6	-	-	1.09		36	1.5
	22	50	30.1 d = 34.8	[3]	H_1	44%	-	-	24.2	34.8	1.07	40	63	2.8
	32	50	31.8 d = 36.7	[3]	H_1	40%	-	-	24.2	36.7	1.05	40	67	2.9
αManOC$_8$	6	25	24.3	[3]	L_α	51%	12.4	11.9	-	-	1.12		38	1.6
	22	50	28.4 d = 32.8	[3]	H_1	44%	-	-	22.8	32.8	1.07	42	67	2.9
	33	50	30.7 d = 35.4	[3]	H_1	39%	-	-	23.3	35.4	1.04	42	70	3.0
αManOC$_{10}$	5	25	28.2	[3]	L_α	57%	16.0	12.2	-	-	1.08		37	1.6
αManOC$_{12}$	25	50	36.5	[3]	L_α	50%	18.4	18.1	-	-	1.01		39	1.7
	45	50	39.5	[3]	L_α	41%	16.0	23.5	-	-	0.94	45		**2.0**
βMaltoOC$_{12}$	15	75	39.2	[5]	L_α	42%	16.6	22.6	-	-	1.10		45	**2.0**

water concentration and drastically increases upon phase transition from a lamellar to a columnar assembly. A look at the layer thicknesses reveals a behaviour similar to the one previously described for branched-chain glycosides; the hydrophobic layer is shrinking with increasing water concentration. However, the effect is less prolonged than the corresponding shrinkage of the sugar domain in branched glycosides. The calculated values for the packing parameter A/A_0 and the observed assembly geometry mostly match the packing theory. The exceptions, highlighted in Table 6, again are due to an underestimation of the reference surface area A_0.

The values for the diameter of the inner (hydrophobic) cylinder for the columnar lyotropic phase, $2r_C$, exceed the size of two all-trans configurated alkyl chains. Considering bond lengths l_{C-C} = 1.54 Å, l_{C-H} = 1.11 Å, l_{C-O} = 1.41 Å and bond angles of 109.5̊, the maximum length of an octyl chain is:

$$L_{max} = \sin\left(\frac{109.5^\circ}{2}\right)\left(7 \times 1.54 + 1.11 + \frac{1.41}{2}\right). = 10.3\text{Å} \quad (16)$$

Assuming a non-bonding distance of about 2 Å, the diameter for the hydrophobic domain cannot exceed 22.5 Å. However, all calculated values in Table 6 are larger. While the deviations for the α-mannoside may be considered acceptable within experimental precision, this does not apply for the β-glycosides βGlcOC$_8$ and βGalOC$_8$, which exceed the theoretical maximum by about 10%. It shows that the assumption of a smooth circular shaped cylinder for the hydrocarbon domain is wrong; hence the interface area per molecule is underestimated. With respect to the volume fraction, an elliptical cylinder with an axial ratio of about 4:5 could be considered, according to:

$$\varphi_C \; d_0^2 \frac{2}{\sqrt{3}} = \pi ab = \pi L_{max} \; b. \quad (17)$$

However, due to the significant deviation from circular shape, one should expect a deformation of the hexagonal structure, probably leading to a tetragonal columnar assembly instead. More likely is the expression of surface roughness. Sterical packing constraints for the sugar head-groups seem to impede the formation of the smooth cylinder interface. In this way, sugar-based surfactants exhibit different assembly behaviour than conformational more flexible polyethylenoxide analogues. It is expected that the surface roughness diminishes with increasing water concentrations, due to better packing flexibility based on the mobility of water molecules.

The sharp increase of molecular surface area upon phase transition from a lamellar to a columnar assembly, Figure 3, suggests a drastic change in the structure of the corresponding compounds. However, it does not refer to the molecular structure, but to the assembly. The molecular surface area of a compound changes drastically upon heating near the phase transition temperature. This, however, does not correspond with a significant increase in the domain interface as shown in Figure 3. Unlike the molecular surface area, the interface of domains shows a

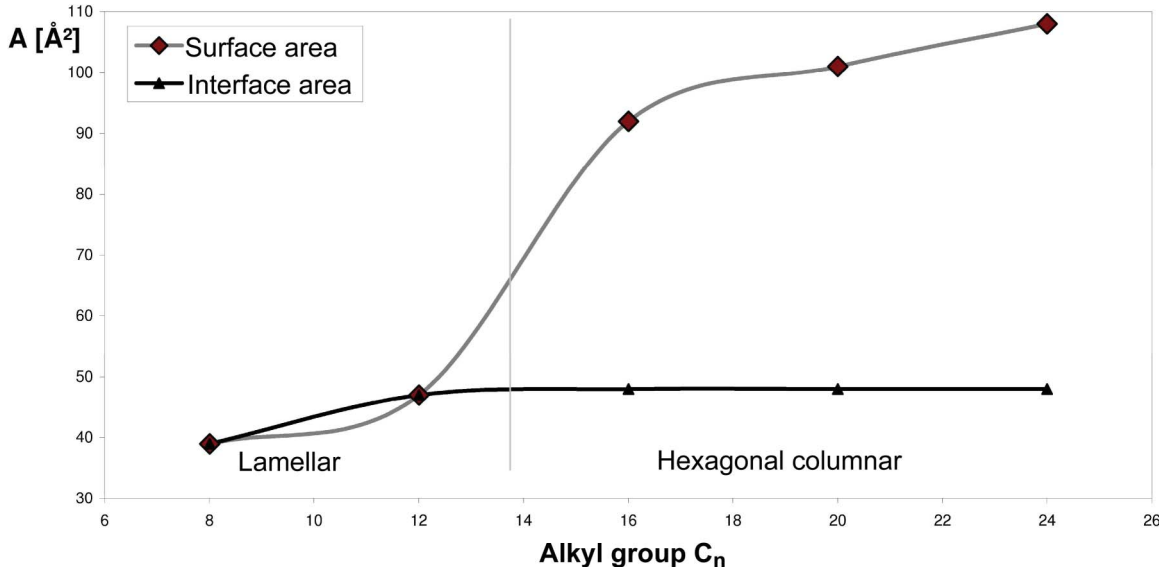

Figure 3. Molecular surface and domain interface area for branched chain β-glucosides as a function of the alkyl group size.

continuous gradual increase with temperature, chain length and water concentration regardless of phase transitions (Tables 3, 4 and 6).

4. Theoretical explanation

The increase of the number of carbon atoms in the chain of branched alkyl glycosides decreases the packing efficiency in the chain region, causing the distance between lipids to increase, hence the surface area per molecule increases. The increasing surface area of the chain region reduces packing stress in the sugar domain within the lamellar phase. This relaxation will develop to the point where constraints occur in the hydrophilic domain due to increased spacing of the sugars, which would create a 'vacuum' if the lamellar phase is maintained. This can be described using the equation below, representing the force, f, between head groups at a distance, l, in the lamellar phase based on the assumption an elastic force constant k.

$$f = -k(l - l_{\mathrm{r}}). \tag{18}$$

The distance l_{r} represents the minimum of elastic energy. For straight and short-branched alkyl chains, $l \leq l_{\mathrm{r}}$ indicates packing stress for the hydrophilic domain. This may result in the formation of a hexagonal phase, H_{I}, as demonstrated for lyotropic formulations. With increasing ratio of volume and length of the hydrophobic domain, the distance l increases, first stabilising the lamellar assembly but then creating packing constraints inside the hydrophobic region, when $l \leq l_{\mathrm{r}}$. This leads to the formation of a columnar phase H_{II}. The work done by the surface tension in the head region, which increases due to the increase of the surface area per molecule, will contribute to the free energy of curvature.

According to Tables 3 and 6, β-glucosides form lamellar assemblies up to a molecular surface area of about 50 Å^2, while columnar assemblies are observed above this figure. Assuming a cylindrical or conical shape of the molecules, the molecular surface area can be converted into the molecular distance l_r in Equation (19) according to:

$$l_{\mathrm{r}} = \sqrt{\frac{4A}{\pi}} = 8\text{Å}. \tag{19}$$

The corresponding value for β-maltosides is larger ($\geq$70 Å^2), leading to a stress-free distance of $l_{\mathrm{r}} \geq 10$ Å.

The free energy per unit area of the curving lipid layer is given by the Helfrich's equation [20] as follows:

$$E = \kappa_1 (H - H_0)^2 + \kappa_2 K, \tag{20}$$

where E is the curvature elastic energy per interface area, H is the mean curvature, H_0 is called the spontaneous mean curvature, K denotes the Gaussian curvature, and κ_1 and κ_2 are the respective bending rigidities. The free energy of the curvature can be a measure for the tendency of the lipid layer to curve. Increasing free energy results in reduced tendency of the layer to bend [21]. For a columnar structure $K = 0$ and the mean curvature of the cylinder is:

$$H = \frac{1}{2R}, \tag{21}$$

where R denotes the radius of the cylinder that depends on the length of lipids. As the length of the lipid molecule increases due to the increasing number of carbons in the hydrocarbon chain, the mean curvature of the cylinder formed by those molecules becomes smaller and the curvature free energy reduces. This might be the reason why βMaltoOC$_{14}$2C$_{10}$ forms the inverse columnar phase at lower temperature than βMaltoOC$_{12}$2C$_{8}$ (see Table 4).

5. Conclusion

The geometry of glycoside assemblies is related to the molecular surface area of the surfactant molecules. The different behaviour of branched and straight-chain glycosides results from the differences in the ratio of the volume and the length of the hydrophobic domain. Increase of the volume length ratio of either hydrophilic or hydrophobic region increases the tendency for the formation of a columnar phase. This enables the prediction of trends for the assembly behaviour of glycolipids based on molecular structure comparisons. However, the molecular surface area is significantly affected by the geometry of the assembly. Hence, simple molecule-based estimations of domain surface areas cannot be used to predict the phase of a glycolipid accurately.

Acknowledgements

This work was supported by the Malaysian Ministry of Science, Technology and Innovation under the HCD-EXPT program and e-Science grant 03-01-03SF0083/13-02-03-3021, as well as by the University of Malaya under research grant FS349/2008A.

References

[1] Kitamoto, D.; Isoda, H.; Nakahara, T. *J. Biosci. Bioeng.* **2002**, *94*(3), 187–201.
[2] Barón, M. *Pure Appl. Chem.* **2001**, *73*(5), 845–895.
[3] Sakya, P.; Seddon, J.M.; Vill, V. *Liq. Cryst.* **1997**, *23*, 409–424.
[4] (a) Vill, V.; Boecker, T.; Thiem, J.; Fischer, F. *Liq. Cryst.* **1989**, *6*, 349–356. (b) Vill, V.; von Minden, H.M.; Koch, H.H.J.; Seydel, U.; Brandenburg, K. *Chem. Phys. Lip.* **2000**, *104*, 75–91. (c) Vill, V.; von Minden, H.M.; Koch, H.H.J.; Seydel, U.; Brandenburg, K. *Chem. Phys. Lip.* **2000**, *106*, 157–179.
[5] Auvray, X.; Petipas, C.; Louvet, S.; Anthore, R.; Rico-Lattes, I.; Lattes, A. *Eur. Phys. J. E* **2001**, *4*, 489–504.
[6] Hashim, R.; Hassan, H.; Mohd Rodzi, N.Z.; Duali Hussen, R.S.; Heidelberg, T. *Thin Solid Films* **2005**, *509*, 27–35.
[7] Abeygunarate, S.; Hashim, R.; Vill, V. *Phys. Rev. E: Stat., Nonlinear, Soft Matter Phys.* **2006**, *73*, 011916.
[8] Vill, V.; Hashim, R. *Curr. Opin. Colloid Interface Sci.* **2002**, *7*, 395–409.
[9] Hassan, S.; Rowe, W.; Tiddy, G.J.T. Surfactant liquid crystals. In *Handbook of Applied Surface and Colloid Chemistry Vol. 1*: Holmberg, K., Ed.; John Wiley: Chichester, 2001; Chapter 21, pp 465–508.
[10] Duesing, P.M.; Templer, R.H.; Seddon, J.M. *Langmuir* **1997**, *13*, 351–359.
[11] Sadoc, J.F.; Charvolin, J. *J. Physique II* **1986**, *47*, 683–691.
[12] Israelachvili, J.N. *Intermolecular and Surface Forces*; Academic Press: London, 1992.
[13] Israelachvili, J.N.; Mitchell, D.J.; Ninham, B.W. *J. Chem. Soc. Faraday Trans. II* **1976**, *72*, 1525–1568.
[14] Jones, J.W.; Lue, L.; Salani, A.; Tiddy, G.J.T. *Liq. Cryst.* **2005**, *32*, 1465–1481.
[15] Lide, D.R., Ed. Physical constants of organic compounds. In *Handbook of Physics and Chemistry*, 10th ed.; CRC Press: New York, 1992.
[16] Zuritz, C.A.; Muñoz Puntes, E.; Mathey, H.H.; Pérez, E.H.; Gascón, A.; Rubio, L.A.; Carullo, C.A.; Chernikoff, R.E.; Cabeza, M.S. *J. Food Eng.* **2005**, *71*, 143–149.
[17] Tukur, N.M. Density-temperature Behavior of Pure and Defined Binary and Ternary Hydrocarbon Mixtures. MSc Thesis, King Fahd University of Petroleum & Minerals, Dharan, Saudi Arabia, 1992.
[18] Seddon, J.M.; Cevc, G. Lipid polymorphism: Structure and stability of lyotropic mesophases of phospholipids. In *Phospholipids handbook*: Cevc, G., Ed.; CRC Press: New York, 1993; pp 403–454.
[19] Chong, T.T.; Heidelberg, T.; Hashim, R.; Gary, S. *Liq. Cryst.* **2007**, *34*, 349–363.
[20] Helfrich, W. *Z. Naturforsch. C* **1973**, *28*, 693–703.
[21] Seddon, J.M.; Templer, R.H. *Philos. Trans. R. Soc. London A* **1993**, *344*, 377–401.